Journal of Power Sources, 1 (1976/77) 2

SOME STUDIES ON SODIUM/SULFUR CELLS

R. BAUER, W. HAAR, H. KLEINSCHMAGER, G. WEDDIGEN and W. FISCHER
Brown, Boveri & Cie AG, Central Research Laboratory, Heidelberg (West Germany)
(Received December 15, 1975)

Summary

Some results concerning the evaluation and improvement of the properties of sodium/sulfur cells are reported. The magnesia doped sodium beta alumina used as an electrolyte in this type of cell has a high conductivity and long life. Current collector and container materials with a high corrosion resistance to the Na_2S_4 melt have been found. Several hundred charge–discharge cycles have been obtained with laboratory cells. High rechargeabilities could be achieved in special cells.

Finally it is shown that the technical and economical prospects for traction and load levelling sodium/sulfur batteries are promising.

Zusammenfassung

Es wird über Experimente berichtet, die mit dem Ziel angestellt wurden, die Eigenschaften von Natrium/Schwefelzellen zu ermitteln und zu verbessern. Das als Elektrolyt für solche Zellen benutzte, mit Magnesiumoxid dotierte Natrium Beta Aluminiumoxid besitzt eine hohe Leitfähigkeit und Lebensdauer. Für den Stromabnehmer und das Gehäuse wurden Materialien mit einer hohen Korrosionsbeständigkeit gegenüber einer Na_2S_4 Schmelze gefunden. Laborzellen konnten mehrere hundert mal geladen und entladen werden. In speziellen Zellen wurde eine hohe Wiederaufladbarkeit erreicht.

Zum Schluss wird gezeigt, dass die technischen und wirtschaftlichen Aussichten für den Einsatz von Natrium/Schwefelbatterien bei der Elektrotraktion und für den Spitzenlastausgleich gut sind.

Introduction

Advanced secondary batteries are under consideration for two applications, both of which will possibly have a very big market in the future. Firstly, they may be utilized as power sources for electric vehicles, secondly they may serve as storage devices for load levelling purposes in electrical networks.

For the traction application the battery should have a high energy and power density and the raw materials used to construct the battery should be abundant [1 - 3]. The sodium/sulfur battery is one possible candidate to fulfil these requirements [3 - 6].

For the load levelling application the battery should have a high efficiency, a long life and low cost [7, 8]. Conventional lead acid batteries could possibly be a solution [9], but lead is a relatively rare element. Also other ambient temperature electrochemical systems, for instance redox cells [10] or high temperature systems like $LiAl/FeS_x$ cells [11] or Na/S cells [12, 13] can be considered. The Na/S cell seems to have a good chance of achieving the characteristics necessary for this type of application [14].

It is the aim of the laboratories developing Na/S cells to optimize the properties of the cells in such a way that one or both of the applications should be possible. This means that several of the properties mentioned above, such as high power and energy density, efficiency and long life, should be obtained simultaneously. To achieve this aim it is necessary to develop an electrolyte with a high conductivity and long life, to minimize the corrosion of the cell components and the polarization in the sulfur compartment, and to maximize the rechargeability of the cell. Some experiments to optimize a few of these properties will be described.

Electrolyte

The sodium ion conductivity and the life time of the beta alumina electrolyte should be high. It is known that resistivities as low as 5 Ω cm or even lower can be obtained at 300 °C with lithia stabilized β'' aluminas [6, 15 - 17] or magnesia stabilized β'' aluminas [15, 18]. Recent experiments at Ford show that β'' aluminas with a high lithia content degrade faster in sodium/sodium cells than β'' aluminas with a low lithia content [6, 19]. Lazennec *et al.* [5] observed that magnesia stabilized beta aluminas are much worse with respect to degradation in sodium/sodium cells than beta aluminas containing only Al_2O_3 and Na_2O. Moreover, the conductivity of pure sodium beta alumina is much lower than the conductivity of beta aluminas containing dopants such as Li_2O or MgO [5, 20, 21]. Therefore it seems that one has to make a compromise between a high conductivity associated with a short life time at high dopant concentrations or a low conductivity associated with a long life time at low dopant concentrations. In order to prove whether this assumption is true or not, beta aluminas of different compositions were prepared and their properties were examined.

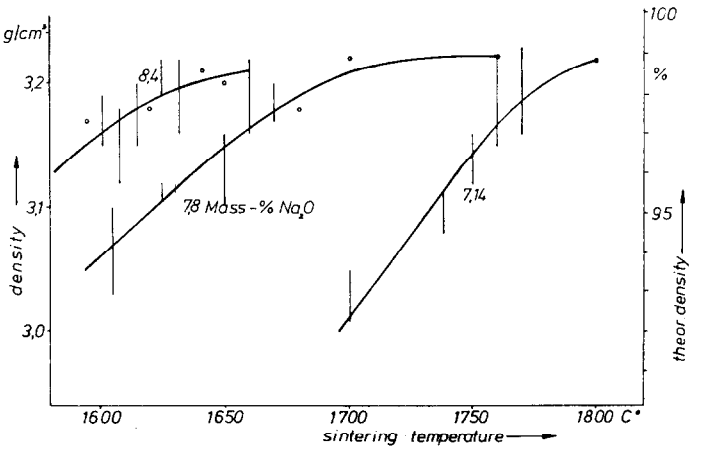

Fig. 1. Density of beta aluminas of different compositions as a function of sintering temperature. Sintering time 0.5 h; MgO content 1 - 4.5 wt.%.

Magnesia was chosen as stabilizer. The composition was varied from 85.5 to 93 wt.% Al_2O_3, 7 to 10 wt.% Na_2O and 0 to 4.5 wt.% MgO. All ceramics were prepared in the same manner: mixtures of anhydrous Na_2CO_3, MgO and α Al_2O_3 were calcined at 1230 °C for one hour and ball milled for twenty hours with 0.5 wt.% ethylene glycol as grinding aid. An additional amount of 0.5 wt.% ethylene glycol was utilized as pressing aid. The powder was isostatically pressed at 1.5×10^3 kg/cm^2. The samples were sintered in a special furnace with a graphite heater element. During sintering the test specimens were embedded in coarse grained β Al_2O_3 powder in order to prevent sodium losses.

In order to obtain electrolytes with a high density it was necessary to determine the density as a function of the sintering temperature and sintering time. The maximum temperature (sintering temperature) was maintained for 0.5 h in all cases. Heating and cooling rates amounted to 15 °C min^{-1}. An annealing period of 1 h followed the sintering process in order to get a better homogeneity and conductivity of the ceramic.

The results of the density measurements are presented in Fig. 1. The bulk densities for beta alumina specimens with three different sodium contents are plotted against the sintering temperature. The bars indicate the spread of the density values resulting from different MgO contents for different sintering processes. The diagram shows that the density tends to a maximum value with increasing temperature for each sodium content.

The resistivity was measured on rods of 30 mm length and 7 mm diameter with a four electrode a.c. technique in the frequency range from 100 Hz to 100 kHz [22]. Graphite contacts were used as electrodes because they are easy to apply and because we could obtain reproducible results in this way [23].

In Figs. 2 and 3 the results of the resistivity measurements at 300 °C on electrolytes with 7.8 and 8.4 wt.% Na_2O are presented together with the

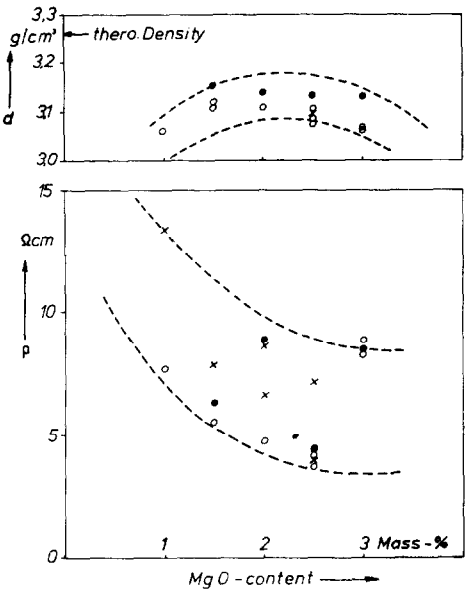

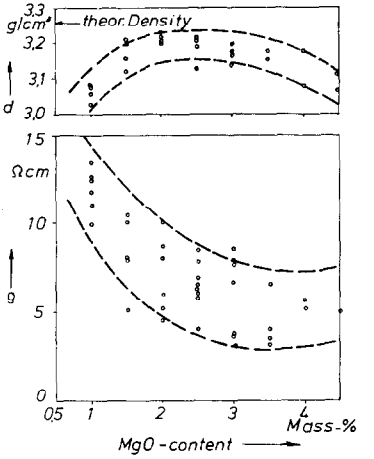

Fig. 2. Influence of MgO content on density d and resistivity ρ at 300 °C of beta aluminas with 7.8 wt.% Na_2O.

Fig. 3. Influence of MgO content on density d and resistivity ρ at 300 °C of beta aluminas with 8.4 wt.% Na_2O.

density measurements. The diagrams show that the resistivity reaches a minimum value asymptotically and that the density passes through a flat maximum with increasing MgO content. Resistivity values as low as 3 Ωcm have been obtained. A decrease in resistivity with MgO content is correlated with an increase in the β'' Al_2O_3/β Al_2O_3 ratio in the ceramic. It is not clear whether the maximum in density is an effect depending on the structure or on the production parameters of the electrolyte.

It has already been shown by other investigators, that not only the density and resistivity, but also the microstructure depends on the composition and the sintering temperature of the ceramic [6, 18, 19, 24].

Figure 4 shows, for a ceramic with 88.6 wt.% Al_2O_3, 8.4 wt.% Na_2O and 3 wt.% MgO, how the texture of the ceramic changes with increasing sintering temperature. Small grains with diameters below 5 μm are produced below 1595 °C. At medium temperatures a duplex structure arises, which means that large crystals coexist with a fine grained matrix. At even higher temperatures the large crystals grow at the expense of the small grains. At the highest sintering temperature the large crystals have lengths of 200 μm and more. Ceramics of this latter type exhibit high densities.

Life tests are being carried out in Na/Na cells. Sodium is electrolysed unidirectionally into the interior of closed-end electrolyte tubes. It flows back into the outer compartment across an isolating collar made of potassium-free glass. A current density of 0.9 A cm^{-2} has been arbitrarily chosen. The

Fig. 4. Change of microstructure of beta alumina (2.5 wt.% MgO; 8.4 wt.% Na_2O) with sintering temperature.

current density in sodium/sulfur cells is usually smaller than this value by a factor of 4. A survey of our recently started tests is given in Table 1.

None of the tubes still being tested have shown any change in resistivity apart from an initial decrease. This initial decrease occurs until the surface of

TABLE 1

Life tests of beta alumina tubes in Na/Na cells[1]

Tube No.	Composition [mass %] (balance Al_2O_3)		Resistivity ρ at 300 °C (Ωcm)	Charge passed through (Ah cm^{-2})	Remarks
	Na_2O	MgO			
1	8.4	1.5	8.6	225[2]	
2	8.4	1.5	8.5 → 5.7	572	terminated because of decrease of ρ
3	8.4	1.5	8.9	660[2]	
4	8.4	1.5	9.0	165[2]	
5	8.4	2.5	5.0	270	terminated because of power failure
6	8.4	3.0	6.5	300	terminated because of power failure
7	9.3	1.0	11.6	280[2]	
8	9.3	1.5	7.9	310[2]	
9	9.3	3.3	4.9	280[2]	
10	9.3	4.0	5.5	165[2]	
11	7.8	0.5 Li_2O	8.3	280[2]	

[1] Densities 3.15 - 3.20 g cm^{-3}; current density 0.9 A cm^{-2}; temperature 300 °C.
[2] Still on test, ρ = constant all the time.

the electrolyte is wetted with liquid sodium. We assume that even more charge can be put through because of the constancy of the resistivity. The resistivity calculated from the current, voltage and shape of the tubes is also given in the Table. By comparison it can be seen that these values fall into the range of Fig. 3.

Two of the tests (nos. 5 and 6) failed after some time because of malfunctioning of the power supply. Tube 2 showed a slight decrease in resistivity with time. After dismantling the tube showed small cracks. Tube 2 was sintered at a relatively high temperature so that coarse grains had developed. Other tubes with grains up to 300 μm showed an even faster degradation. Tubes sintered at a relatively low temperature, which were fine grained but had some open porosity, degraded from the beginning of the test. During the passage of a charge of 20 Ah cm^{-2} the resistivity decreased by a factor of 2 to 5.

It can be concluded from these preliminary results that the production procedure and especially the sintering process has to be carefully optimized with respect to the microstructure and the porosity of the ceramic. There is no indication as yet that the long life depends on the composition of the electrolyte within the limits of the compositions investigated. The negative results of other investigators with respect to the long life of MgO stabilized ceramics [5] could not be confirmed by our experiments. Whether there are differences in stability over a longer period of time is subject to further investigation. For the present it must be concluded that the conductivity and the life time can be optimized separately.

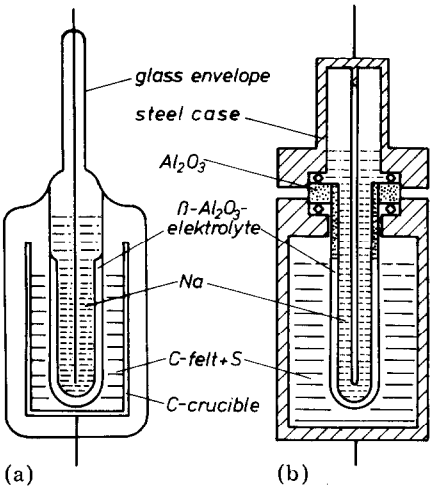

Fig. 5. Sodium/sulfur cells used for most of the experiments. (a) Metal free cell with glass container; (b) cell with steel case current collector.

Corrosion experiments

One of the main problems in realizing a sodium/sulfur battery with a long life is to avoid or to retard the corrosion of the container material by sodium polysulfides. Figure 5 shows a Na/S cell in which the container acts also as a cathodic current collector. This means that chemical as well as electrochemical corrosion may take place at the container surface in contact with the sodium polysulfide melt.

Na/S cells must not necessarily be constructed in the way shown at the right hand side of Fig. 5. An additional graphite current collector, which does not corrode in sodium polysulfide, can be used. In this way the electrochemical corrosion of the container material would be avoided. However, the energy density will be decreased because of the additional component within the cell. Another solution of the corrosion problem consists in exchanging the sodium and the sulfur, so that the sulfur is contained in the tubular ceramic electrolyte. In this way the cover of the upper end of the electrolyte tube would be the only part which is exposed to evaporating sulfur or eventually to liquid polysulfide. This cover could, if necessary, be made of an expensive material. From a safety point of view, it is desirable to have the sodium in the inner part of the cell. Therefore a type of cell similar to that of Fig. 5 seems to be the best solution, if corrosion resistant container and current collector materials can be found.

A screening program was initiated in order to find such materials. For this purpose samples of different materials (see Table 2) with a weight of several grammes were introduced in glass ampoules together with Na_2S_4. All operations were performed in an inert gas atmosphere. After filling, the ampoules were evacuated, melted off and held at a temperature of 320 °C for

TABLE 2

Chemical composition (wt.%) of alloys investigated

Material no.	Ni	Cr	Fe	Co	Al	Other elements
1	4.9	18.4	bal.	—	—	3.7 Mo; 0.03 C; 1.6 Si; 1.5 Mn
2	4.5 - 6.5	21 - 23	bal.	—	—	2.5 - 3.5 Mo; ⩽ 0.03 C; 0.08 - 0.2 S
3	11.5	18	bal.	—	—	0.06 Ti; 2.2 Mo; ⩽ 0.01 C
4	13	18	bal.	—	—	2.8 Mo; ⩽ 0.07 C
5	12.5 - 14.5	21 - 23	bal.	—	—	4.0 - 5.0 Mo; ⩽ 0.04 C; ⩽ 1.0 Si; ⩽ 2.0 Mn
6	bal.	18 - 21	<5	<2	1.2 - 1.8	1.8 - 2.7 Ti; ⩽ 0.1 C
7	bal.	15.5	1.0	10.0	4.25	1.75 Ti; 1.75 Mo; 3.5 W; 0.15 C; 1.75 Nb
8	bal.	23	14.1	—	1.35	0.05 C; 0.5 Mn
9	bal.	23.8 - 24.8	<0.5	19.0 - 20.5	1.2 - 1.6	2.8 - 3.2 Ti; 1.2 - 1.7 Mo; 0.03 - 0.07 C
10	9.5 - 10.5	23.5 - 24.5	<0.5	bal.	—	0.15 - 0.25 Ti; 6.5 - 7.5 W; 0.55 - 0.65 C

a time of (in most cases) 500 h. Previous experiments had shown that the corrosion rate of Duran glass (Schott, Mainz), which was used for the ampoules, is negligible. Na_2S_4 was synthesized by the reaction of sodium in ethanol with H_2S and sulfur to a Na_2S_4 solution in three steps. The ethanol was driven out by vacuum evaporation. Na_2S_4 produced by this method is very pure. Details of the method will be described elsewhere [25].

After the corrosion treatment Na_2S_4 adherent to the specimens was dissolved in ethanol. The corrosion phenomena were investigated by weight, scanning electron microscopy, metallographic, microprobe and X-ray diffraction analysis. The results are summarized in Table 3 overleaf.

On stainless steels and superalloys a duplex sulfide layer is formed. The outer layer is rich in the base element and the inner layer rich in the alloying element, which is chromium in all cases. Similar effects have been found at higher temperatures [26, 27].

A cross-section of sample 9 showing these two layers and the distribution of the elements is shown in Fig. 6. Additionally the chemical composition of the two layers is illustrated by the microprobe analysis of the corresponding surface areas (Fig. 7).

It seems to be typical for the corrosion mechanism that the base elements diffuse through the inner layer (mostly thio-spinels) to form well defined pyrite crystals. Two examples of the morphology of corroded surfaces are shown in Figs. 7 and 8.

The corrosion rate of superalloys is smaller than that of stainless steels because of the probable lower diffusivity of nickel and cobalt compared with iron.

Local pitting or intercrystalline corrosion was observed respectively, when zirconium or molybdenum were used.

It can be concluded from the experiments, that the corrosion rate of the superalloys tested is about ten times lower than the corrosion rate of stainless steels. Further investigation will show whether the corrosion behaviour of these materials allows their use under the conditions found in Na/S cells.

Cell tests

Many papers have been published on the performance of sodium/sulfur cells. Recent publications show that high discharge current densities can be achieved at high efficiencies and that many charge–discharge cycles can be obtained with laboratory cells [6, 12, 28 - 31]. But the rechargeability (charging from Na_2S_3 to S corresponds to 100%) is low at higher current densities with cells in which the sulfur compartment is close-packed with a graphite felt [4, 6, 12]. It has been shown that introducing convection holes in the graphite felt electrode, changing the wettability by using other felt materials [6] and utilizing a non-conducting diaphragm between the electrolyte and the graphite felt [12, 30] increases the rechargeability.

TABLE 3

Selected corrosion data; 500 h at 320 °C in Na_2S_4 melt

Material	Wt. change (mg cm^2)	Morphology of the corrosion layer	Thickness of inner (a) and outer (b) layer (μm)	Corrosion products
1	+3.36	duplex sulfide layer inner layer: compact Cr enriched scale; no sulfur diffusion at the scale–metal interface outer layer: coarse grained crystallites with octahedral habits; mainly Ni–Fe pyrites	a 1.4 - 4 b - 30	(Ni, Fe) Cr_2S_4 $Fe_{0.93}$ $Ni_{0.07}$ S_2
2	+2.01		a 1 - 4 b 10 - 30	thio-spinels Fe_x Ni_{1-x} S_2
3	+3.10		a 4 b 4 - 16	(Ni, Fe) Cr_2S_4 $Fe_{0.78}$ $Ni_{0.22}$ S_2
4	+2.41		a 2 - 6 b - 20	thio-spinels Cr_3S_4 ? Fe_x Ni_{1-x} S_2
5	+2.14		a 2 - 5 b - 20	(Ni, Fe) Cr_2S_4 $Fe_{0.71}$ $Ni_{0.29}$ S_2
6	—0.11	duplex sulfide layer inner layer: same as 1 - 5 outer layer: mostly microcrystalline; crystallites partly octahedral; partly cubic or irregular	a not det. b 1.3 - 2.5	thio-spinel ? pyrite: a_0 = 5.678 Å
7	+0.15 - 0.27		a not det. b - 2.5	chromium sulfide pyrite: a_0 = 5.650 Å
8	—0.01		a 0.5 - 0.75 b 5 - 7	thio-spinel: a_0 = 9.47 Å pyrite a_0 = 5.635 Å
9	+0.23 - 0.86		a - 1.5 b - 5	thio-spinel: a_0 = 9.41 Å pyrite: a_0 = 5.617 Å
10	+0.22 - 0.40		a not det. b not det.	thio-spinel: a_0 = 9.5 Å pyrite: a_0 = 5.578 Å
Cr	—2.85	multi-scale with different Cr content	10 - 38	Cr $S_{1.38}$
Zr	—0.88	local pitting, 20 - 30 μm	max. 0.1	—
Mo	+1.15	intercrystalline corrosion, no layers	—	—

Two types of cells which we used for many of our experiments are presented in Fig. 5. The metal-free type at the left hand side contains graphite felt between a closed-end beta alumina tube and a graphite crucible current collector. A molybdenum wire and a nickel/chromium/iron alloy wire were used as cathodic and anodic terminals respectively. Oxygen-free sodium and sulfur are introduced by an inert gas filling technique. Finally the compartments are evacuated and sealed off.

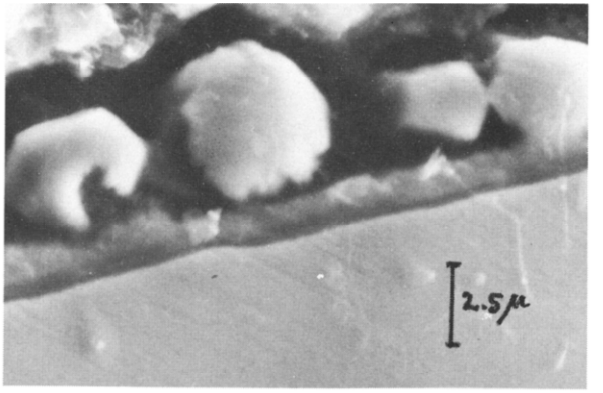

(Ni + Co) pyrite
Cr sulphides

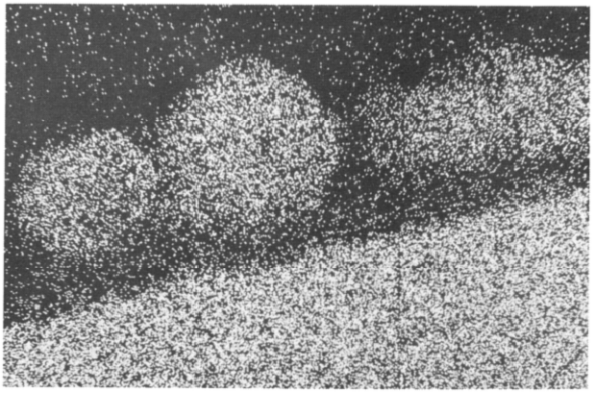

Ni

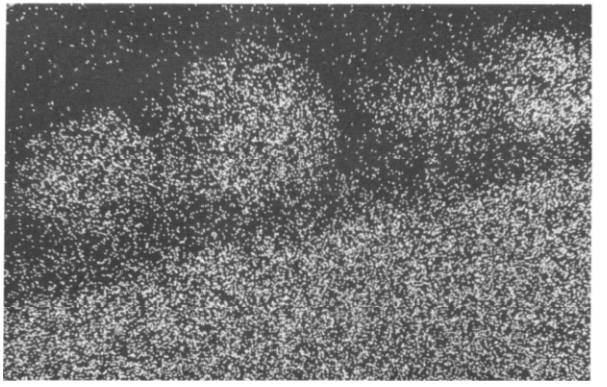

Co

(Fig. 6. For caption, see overleaf.)

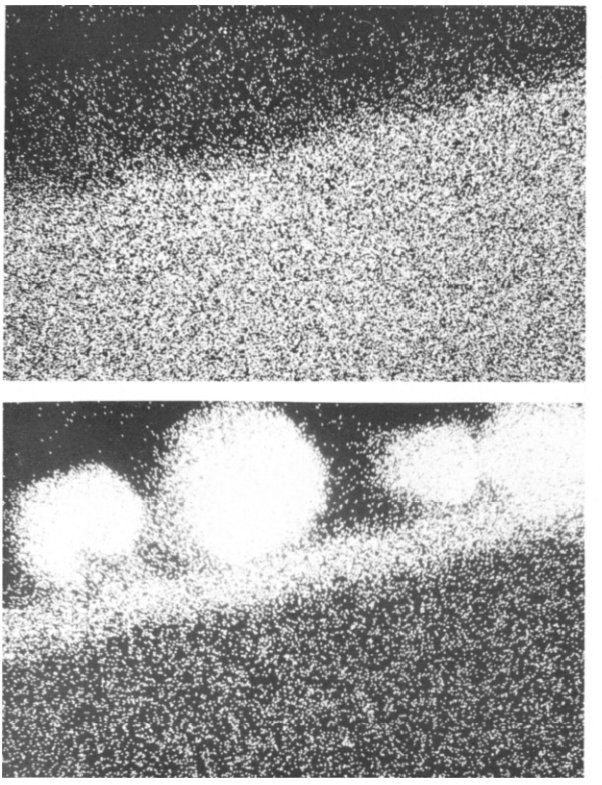

Fig. 6. Cross-section and element distribution of sulfide scale formed on nickel-based alloy No. 9 after 500 h exposure at 320 °C to Na_2S_4-melt.

In the type of cell presented on the right hand side of Fig. 5 the stainless-steel case is also used as cathodic current collector. The tubular electrolyte is connected to an alpha alumina collar by a glass seal. Metallic gaskets are used to accomplish a compression seal, by which the two compartments are separated from each other and from the atmosphere. The cells were filled in a similar way to the metal-free cells.

The cells could be discharged at 300° and 350 °C with high current densities, up to 300 mA cm^{-2}. The cell voltage–discharge time curve shows a plateau, which coincides with the two-phase region of the Na–S phase diagram. After that the cell voltage decreases (one phase region). At low current densities (10 - 15 mA cm^{-2}) the rechargeability was high in many cases (up to 90%) with the two phase regions again clearly distinguishable. At higher charge current densities the rechargeability decreased. Very similar results have been obtained in other laboratories [6]. From the shape of the cell voltage–recharge time curve, and with the aid of reference electrodes, it could be shown that the cells were only recharged in the homogeneous (Na_2S_3–Na_2S_5) phase region.

In order to prove whether the rechargeability can be increased, experiments were started with cells which can be disassembled easily. These are

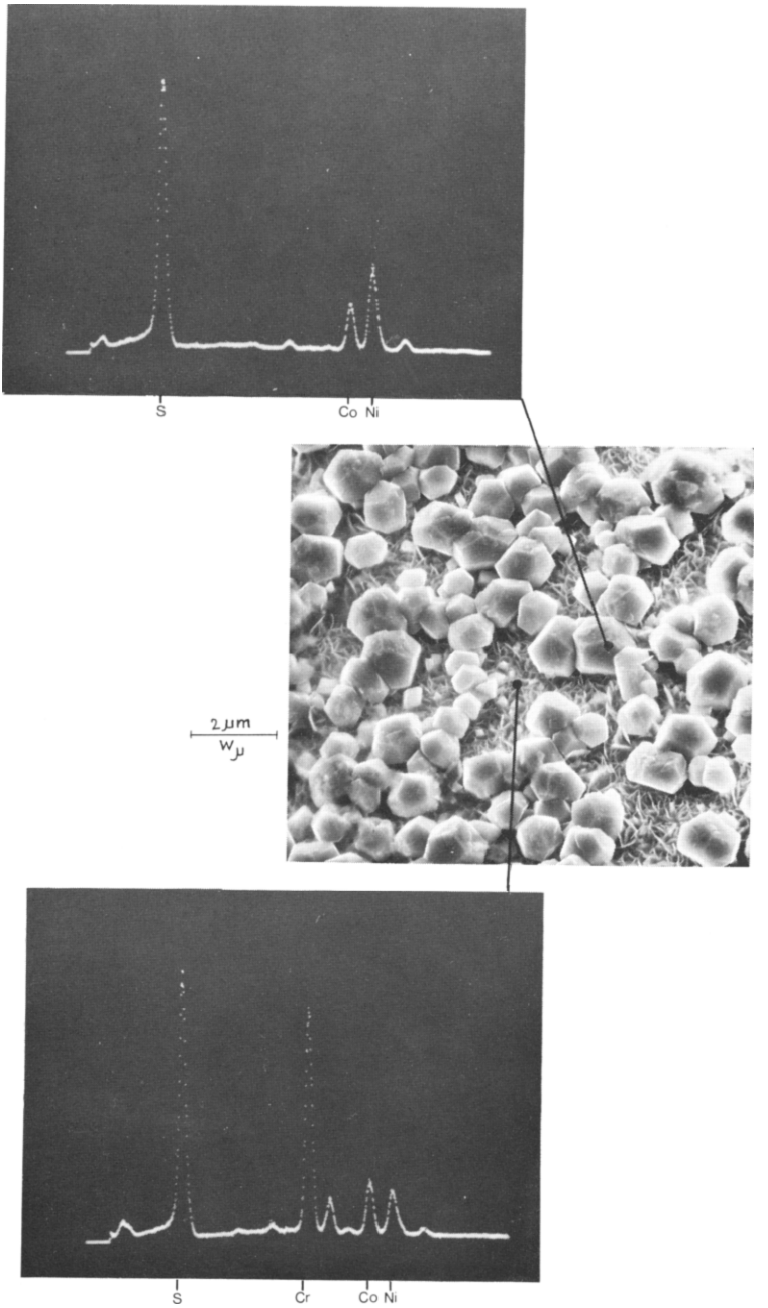

Fig. 7. Morphology and microprobe analysis of the surface of the nickel-based alloy No. 9 corroded in Na_2S_4.

similar to the cell shown at the left hand side of Fig. 5, but they have a ground-glass joint at the upper end of the sulfur compartment. Sodium is filled into the interior of the beta alumina tube by electrolysis of a $NaNO_3$ melt

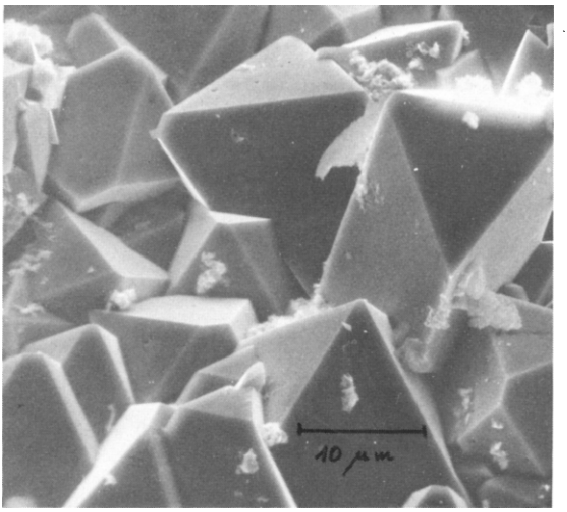

Fig. 8. Surface morphology of stainless steel No. 4 after 500 h exposure at 320 °C to Na_2S_4 melt.

The materials within the cathode compartment and the configuration of the sulfur electrode can be changed quickly with this cell design. An inert gas atmosphere is maintained within the cathode compartment and around the cell in the furnace.

The results of our first experiments at 300 °C are summarized in Table 4. The cells had been discharged down to a Na/S ratio of 2:3. They were recharged at a current density of 40 mA cm^{-2}. Rechargeability values could be reproduced within ±2%, with the exception of cell 3.

According to Table 4 the rechargeability of the standard cell (no. 1) was low. It could be increased by changing the shape of the felt and the composition of the melt. The rechargeability of the shaped graphite felt cell (no. 2) is higher by a factor of 1.7 than the rechargeability of the standard cell, but it is lower than the rechargeability observed at Ford [6]. This may be due to differences in the dimension of the holes within the felt. As a result the electrode kinetics may be influenced by convection of the melt to a different extent. The increase in rechargeability resulting from additives may be due to a change in the wetting properties of the melt and/or to a shortening of the chain length of the sulfur. As a consequence of the latter effect the viscosity of the melt and/or the kinetics of the electrochemical reactions may be changed.

A relatively high rechargeability has been obtained by adding selenium to the sulfur. At a charging current density of 20 mA cm^{-2} it increased to 82%, at 120 mA cm^{-2} it was still 52%.

An even higher rechargeability could be obtained, when both holes and additives had been applied (cell no. 6). But it is not yet certain if this is due to a superposition of both effects, or to the fact that the sulfur compartment of cell no. 6 had been evacuated. Higher rechargeabilities have been observed

TABLE 4

Dependence of the rechargeability on sulfur electrode parameters (300 °C, 40 mA cm^{-2})

Cell no.	First line: Composition of cathode material Second line: Material and configuration of felt	Rechargeability (%)
1	sulfur graphite felt	38
2	sulfur graphite felt with vertical holes at electrolyte tube	66
3	sulfur + ~1 mol % B_2S_3 graphite felt	64
4	sulfur + ~1 mol % P_2S_5 graphite felt	42
5	sulfur + ~1 mol % Se graphite felt	75+
6*	sulfur + ~1 mol % Se graphite felt with vertical holes at electrolyte tube	85++

*Cell with metal case (Fig. 5)
+52% at 120 mA/cm^2
++68% at 65 mA/cm^2

also in evacuated standard cells compared with those operating in an inert gas atmosphere. The reason for this effect is not known (for a possible explanation see ref. [6]).

Several cells with a steel case current collector have been set in operation in order to evaluate their longtime behaviour. Figure 9 shows the capacity of one of these cells as a function of the cycle number and the charging current density. The current density was increased in several steps during the first 50 cycles.

Thereafter the cell was charged at 65 and discharged at 130 mA cm^{-2}. The capacity amounted to only 30% of the theoretical value but it remained constant during about 440 cycles. The test had to be terminated because of a power failure. Chemical analysis of the sulfur compartment showed that the corrosion rate of the steel case current collector was much lower than had been expected from the corrosion tests of Table 3. A cell with increased capacity (no. 6 of Table 4) has been set in operation in order to prove whether the corrosion rate is low in these operating conditions also.

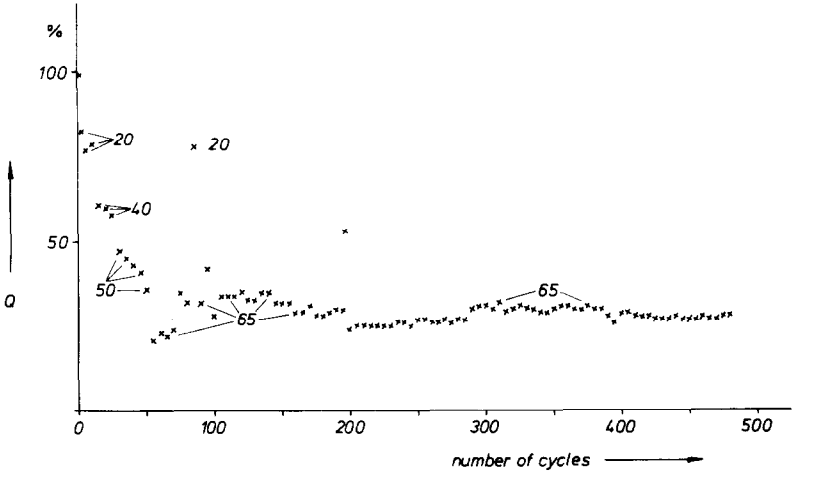

Fig. 9. Ratio Q = capacity/theoretical capacity of a cell with steel case current collector as a function of cycle number. Numbers are charge current densities in mA cm^{-2}.

Application possibilities

It has been mentioned initially that high energy and power density are the most important criteria for the application of batteries for traction purposes. These properties have been estimated for a 50 kWh sodium/sulfur traction battery.

It can be concluded that the thermal insulation, which is necessary to keep a multicell battery at the operating temperature, will have about the same weight as the cells. The energy density of the developed battery including the insulation will be about 100 Wh kg^{-1} for a five hour discharge time. The energy and the power density will be about 4 times higher than the energy and power density of a lead-acid traction battery. Therefore the sodium/sulfur battery will be an attractive energy source for electric vehicles. This conclusion has been drawn before [1 - 4].

The most important properties for the load levelling application are the efficiency, the life time and the cost of the battery. It can be assumed that the life time of fully developed sodium/sulfur batteries will be high for two reasons. First, it can be concluded from the section on corrosion experiments that these problems will be probably solved. Secondly it has been shown in the section on electrolytes that more charge than 660 Ah cm^{-2}, and in other laboratories that 3000 Ah cm^{-2} [6], can be passed through properly produced electrolytes. For a storage device delivering peak power over twenty years, three hours per day, a charge passage of about 2000 Ah cm^{-2} is necessary.

A study has been performed in order to estimate the investment costs of a sodium/sulfur storage plant as a function of discharge time, current density and discharge efficiency. The single cells are constructed similarly to the cell of Fig. 5, but n electrolyte tubes are inserted into one cell.

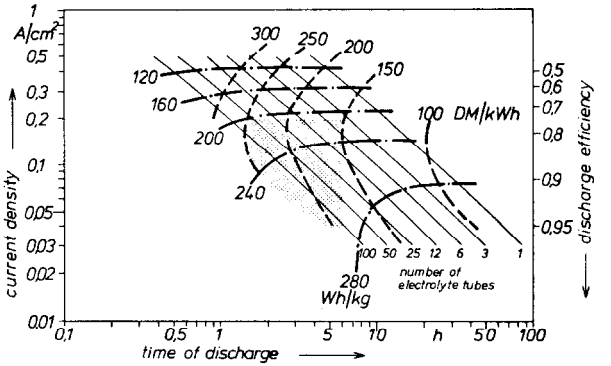

Fig. 10. Estimated interdependence of different properties of sodium/sulfur batteries, built of cells with a maximum energy content (small current density, 100% rechargeability) of 5 kWh. Cells contain several electrolyte tubes. Cost estimations refer to large scale production.

The results are presented in Fig. 10. The diagram shows curves for a fixed number n of electrolyte tubes per cell, for a constant energy density and for constant specific costs c in a plot of discharge efficiency against discharge time t. The area $\eta \leqslant 0.75/c \leqslant 250$ DM kWh^{-1} $/t \leqslant 6$ h is marked by dots. Sodium/sulfur batteries with properties within this area may be used for load levelling applications. Similar properties of sodium/sulfur batteries have been estimated in ref. [4]. It has been shown that batteries with costs and efficiencies in accordance with this estimation can economically compete with conventional peak power plants [7].

Acknowledgement

This work was supported by the German Ministry of Research and Technology (NT 4471 G).

References

1 D. V. Ragone, Review of Battery Systems for Electrically Powered Vehicles, Int. Automot. Eng. Congr., Detroit, Mich., SAE (Soc. Automot. Eng.) [Tech. Pap.] (1968) 680 453.
2 J. Jansta and J. Riba, Elektrotech. Obz., 2 (1973) 88 - 93.
3 W. Fischer, Elektrizitätsverwertung, 49 (1974) 296.
4 J. L. Sudworth, Proc. 10th Intersoc. Energy Conv. Eng. Conf., Newark, De, (1975) 616.
5 Y. Lazennec, C. Lasne, P. Margotin and J. Fally, J. Electrochem. Soc., 122 (1975) 734.
6 S. A. Weiner *et al.*, Research on Electrodes and Electrolyte for Ford Sodium–Sulfur Battery, Ann. Rep. Nat. Sci. Found., (1975), Contract NSF C-805.
7 W. Fischer, Elektrotech. Z., Ausg. A., in press.
8 N. P. Yao, Proc. 10th Intersoc. Energy Conv. Eng. Conf., Newark, De, (1975) 1107.

9 N. J. Maskalick, J. T. Brown and G. A. Monito, Proc. 10th Intersoc. Energy Conv. Eng. Conf. Newark, De, (1975) 1135.
10 K. D. Beccu, Chem. Ing. Techn., 46 (1974) 95.
11 R. O. Ivins, A. A. Chilenskas, V. M. Kolba, W. L. Towle and P. A. Nelson, Proc. 1975 IEEE Southeastcon, Charlotte, N.C., April, 1975.
12 S. P. Mitoff and J. B. Bush, Proc. 9th Intersoc. Energy Conv. Eng. Conf., San Francisco, (1974) 916.
13 L. S. Marcoux, R. R. Sayano, E. T. Seo and H. P. Silverman, Proc. 10th Intersoc. Energy Conv. Eng. Conf., Newark, De, (1975) 624.
14 E. W. Brooman and J. E. Clifford, Batteries for Electric Utility Energy Storage, Ext. Abstr. Electrochem. Soc. Fall Meeting, Dallas, (1975) p. 609.
15 M. A. Dzieciuch and N. Weber, U.S. Pat. 3, 719,531, Dec. 22, 1969.
16 TRW-Report Nr. 20078-6002-RU-00, Development Program for Solid Electrolyte Batteries, Prepared for the Electric Power Research Institute, Oct. 1974.
17 C. E. Youngblood and R. S. Gordon, 77th A. Meet., Am. Ceram. Soc., May 3 - 8, (1975) Washington D.C.
18 L. J. Miles and I. W. Jones, Colloq. Electrolytes for Power Sources, Soc. Electrochem., Brighton, Dec. 1973.
19 G. J. Tennenhouse, R. C. Ku, R. H. Richman and T. J. Whalen, Ceram. Bull., 54 (1975) 523.
20 G. J. Tennenhouse, U.S. Pat. 3,468,719 (Sept. 23, 1969).
21 W. Jones and L. J. Miles, Proc. Br. Ceram. Soc., 19 (1971) 161.
22 W. Fischer and W. Haar, Paper presented at the meeting on Mass Transport in Ceramic Materials, Br. Ceram. Soc., London, Dec 1975.
23 W. Baukal and R. Knödler, J. Appl. Electrochem., 5 (1975) 105.
24 R. W. Powers and S. P. Mitoff, J. Electrochem. Soc., 122 (1975) 226.
25 G. Weddigen, H. Kleinschmager and S. Hoppe, to be published.
26 K. N. Straffor, G. R. Winstanley and J. M. Harrison, Werkst. Korros., 25 (1974) 487.
27 T. Narita and K. Nishida, Oxid. Met., 6 (1973) 181.
28 J. L. Sudworth, M. D. Hames, M. A. Storey, M. F. Azim and A. R. Tilley, in D. H. Collins (ed.), Power Sources 4, Oriel Press, Newcastle-upon-Tyne, (1973) p. 1 - 20.
29 J. L. Sudworth, Proc. 10th. Intersoc. Energy Conv. Eng. Conf., Newark, De, (1975) 616.
30 J. Fally, C. Lasne, Y. Lazennec, and P. Margotin, J. Electrochem. Soc., 120 (10) (1973) 1292.
31 R. J. Bones, R. J. Brook, and T. L. Markin, in D. H. Collins (ed.), Power Sources, Academic Press, London, (1975) p. 539.